



ORIGINAL ARTICLE

Assessment of surgical tumor-free resection margins in fresh squamous-cell carcinoma resection specimens of the tongue using a clinical MRI system

Jan Heidkamp MS¹  | Willem L. J. Weijs MD² |
Adriana C. H. van Engen-van Grunsven MD, PhD³ | Ilse de Laak-de Vries BS³ |
Marnix C. Maas PhD¹ | Maroeska M. Rovers PhD^{4,5} |
Jurgen J. Fütterer MD, PhD¹ | Stefan C. A. Steens MD; PhD¹ |
Robert P. Takes MD, PhD⁶ 

¹Department of Radiology and Nuclear Medicine, Radboud Institute for Health Sciences, Radboud University Medical Center, Nijmegen, The Netherlands

²Department of Oral and Maxillofacial Surgery, Radboud University Medical Center, Radboud Institute for Health Sciences, Nijmegen, The Netherlands

³Department of Pathology, Radboud Institute for Health Sciences, Radboud University Medical Center, Nijmegen, The Netherlands

⁴Department of Operating Rooms, Radboud Institute for Health Sciences, Radboud University Medical Center, Nijmegen, The Netherlands

⁵Department of Health Evidence, Radboud Institute for Health Sciences, Radboud University Medical Center, Nijmegen, The Netherlands

⁶Department of Oto-Rhino-Laryngology and Head and Neck Surgery, Radboud Institute for Health Sciences, Radboud University Medical Center, Nijmegen, The Netherlands

Correspondence

Jan Heidkamp, P.O. Box 9101, internal postal code 766, 6500 HB Nijmegen, The Netherlands.
Email: jan.heidkamp@radboudumc.nl

Section Editor: Martin Hullner

Abstract

Background: Current intraoperative methods of visual inspection and tissue palpation by the surgeon, and frozen section analysis cannot reliably prevent inadequate surgical margins in patients treated for oral squamous-cell carcinoma (OSCC). This study assessed feasibility of MRI for the assessment of surgical resection margins in fresh OSCC specimens.

Methods: Ten consecutive tongue specimens containing OSCC were scanned using 3 T clinical whole-body MRI. Two radiologists independently annotated OSCC location and minimal tumor-free margins. Whole-mount histology was the reference standard.

Results: The positive predictive values (PPV) and negative predictive values (NPV) for OSCC localization were 96% and 75%, and 87% and 79% for reader 1 and 2, respectively. The PPV and NPV for identification of margins <5 mm were 38% and 91%, and 5% and 87% for reader 1 and 2, respectively.

Conclusions: MRI accurately localized OSCC with high inter-reader agreement in fresh OSCC specimens, but it seemed not yet feasible to accurately assess the surgical margin status.

KEYWORDS

margins of excision, MRI, squamous cell carcinoma of head and neck, tongue neoplasms, whole mount histology

1 | INTRODUCTION

Squamous-cell carcinoma of the oral cavity represents 2% of all new cancer cases and is predominantly located in the oral tongue (oral squamous-cell carcinoma [OSCC]).^{1,2} Surgery aiming at complete removal of the tumor including a margin of surrounding uninvolved tissue is the mainstay of treatment in patients with OSCC.^{3,4}

After surgery, several factors adversely affect the oncologic outcome, but only the resection margin is controllable by the clinician. Negative histopathological margins are crucial as patients with close or positive margins are at greater risk of developing local recurrence and may subsequently have worse overall survival.⁵⁻⁹ Most commonly a margin larger than or equal to 5 mm is considered as negative, a margin between 1 and 5 mm as close, and a margin less than 1 mm as positive.^{10,11} Inadequate, that is, close or positive, margins are often an indication for resection or adjuvant (chemo) radiotherapy contributing to costs, morbidity, and reduced quality of life of the patients that are faced with these treatments.^{12,13}

Despite universal recognition of the risks that inadequate resection margins bear, incidence rates are 40% to 50%.^{6,14} This illustrates that the currently employed intraoperative methods of visual inspection and tissue palpation by the surgeon cannot reliably assess the surgical margin status. The diagnostic value of intraoperative histopathological assessment of the resection margins by frozen section analysis (FSA) is limited as it is susceptible to sampling errors.^{15,16}

The use of MRI to assess the *ex vivo* resection specimen may overcome these shortcomings by supporting the surgeon with three-dimensional volumetric information on the freshly resected tissue. Previously, evaluation of resection margins in OSCC specimens has been investigated by employing a 7 T preclinical MRI scanner.¹⁷ A logistically more favorable 3 T clinical whole body MRI scanner is available within our operating room (OR) suite which could also obviate the need for 7 T equipment. Furthermore, the method was optimized to be suitable for an envisioned clinical application. The purpose of this study was therefore to assess the

feasibility of employing a 3 T clinical MRI scanner for the assessment of surgical resection margins in fresh OSCC specimens.

2 | MATERIALS AND METHODS

2.1 | Study population

Approval by the Institutional Review Board and written informed consent from all patients were obtained. Patients with biopsy-proven OSCC and scheduled for surgical resection of the primary tumor with either a sentinel node procedure or neck dissection were consecutively included. Patients scheduled for surgery of recurring cancer were excluded.

2.2 | MRI acquisition

While maintained at the OR complex, fresh OSCC specimens were inked in two different colors for left and right, and positioned on an in-house made Perspex container such that the orientation of the MRI slices were identical to histology (Figure 1). The specimen was immersed in perfluoropolyether (Galden, Solvay Solexis, Thorofare, New Jersey) to eliminate magnetic susceptibility artifacts arising at the air-tissue transition and a gauze pad was used to pin down the specimen to the bottom of the container to prevent it from floating. A bilateral four-channel phased array surface carotid coil (Machnet BV, Roden, The Netherlands) was mounted underneath and on top of the container which was positioned in a 3 T clinical MRI system (Magnetom Skyra, Siemens Healthineers, Erlangen, Germany). Axial T2-weighted (T2W) turbo spin echo (TSE) images using echo times (TE) of 12 and 59 ms, and diffusion weighted spin-echo echo planar images were acquired (Table 1). Apparent diffusion coefficient (ADC) maps were calculated based on acquired *b* values of 0, 100, 500, 1000, and 1200 s/mm² using the standard post processing available on the MRI system. Furthermore, 3D T2W TSE and T1-weighted (T1W) volumetric interpolated breath-hold examination images were

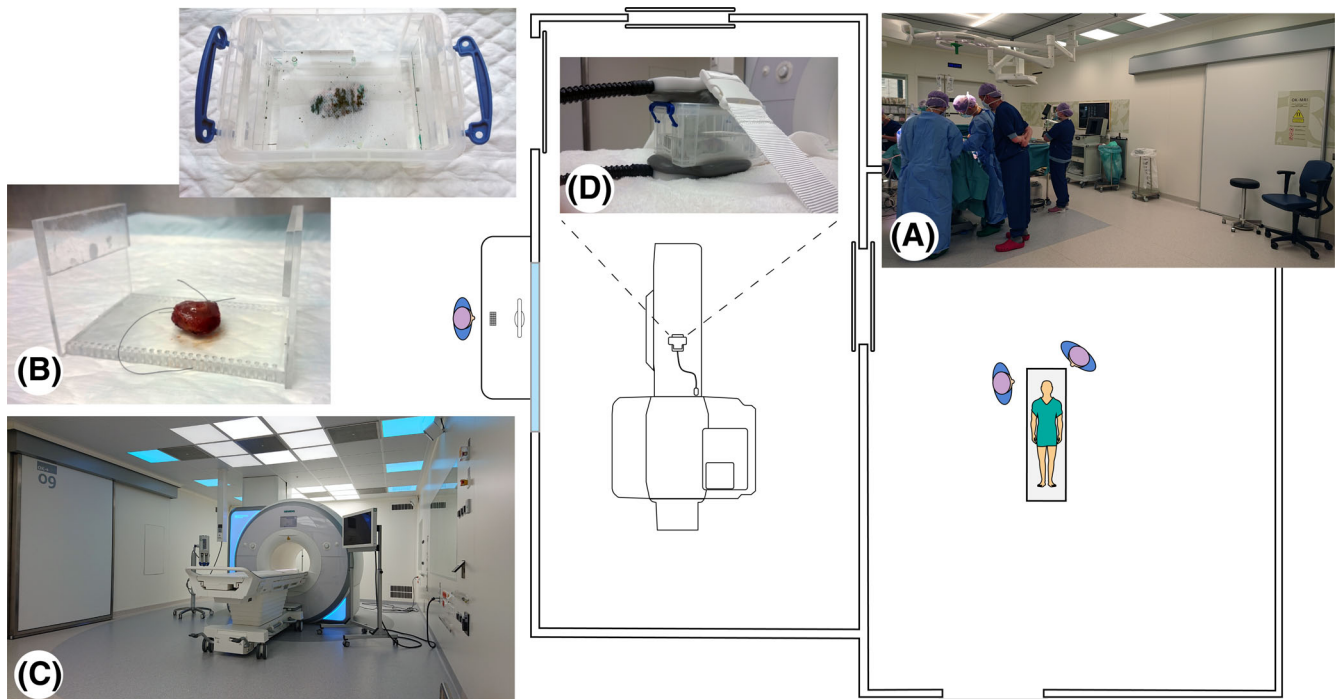


FIGURE 1 Preparation of the surgical specimen for MRI acquisition. A, Partial tongue resection is performed in the operation room adjacent to the MRI room. B, The fresh tongue resection specimen is transported to the pathology minilab where it was inked and positioned on an in-house Perplex container (left inset). The specimen was pinned down to the bottom of the container using a gauze pad and submersed in perfluoropolether (right inset). C, The 3 T clinical MRI system within the operating room suite. D, The container holding the specimen positioned on the MRI table showing the bilateral four-channel phased array surface carotid coil positioned underneath and on top of the container [Color figure can be viewed at wileyonlinelibrary.com]

TABLE 1 MRI sequence parameters

Sequence	No. of slices (min-max)	TR (ms)	TE (ms)	FA (degrees)	ST (mm)	NSA	Voxel size (mm)	Matrix	Scan time (mm:ss)	Echo train length	Readout bandwidth (Hz/Px)
T2W TSE	34	4500	12, 59	150	2	4	0.20	192 × 156	07:01	7	220
DW SE EPI	26	5300	71	90	2	- ^a	0.80	142 × 56	08:18	27	800
3D T2W TSE	72	1500	106	135	0.6	2	0.60	128 × 128	04:10	58	500
T1W VIBE	160	5.5	2.5	11	1	4	0.85	96 × 96	03:26	2	870
SPGR for T1 map	96	7.0	2.60	2, 5, 12, 20	0.8	1	0.80	128 × 88	02:30	1	120
SE for T2 map	1	3000	- ^b	180	5	1	1	64 × 64	03:09	1	300

Abbreviations: DW, diffusion-weighted; EPI, echo planar imaging; FA, flip angle; n/a, not applicable; NSA, number of signal averages; SE, spin echo; SPGR, spoiled gradient echo; ST, slice thickness; T1W, T1-weighted; T2W, T2-weighted; TE, echo time; TIRM, turbo inversion recovery magnitude; TR, repetition time; TSE, turbo spin echo; VIBE, volumetric interpolated breath-hold examination.

^aNumber of signal averages of 1, 3, 6, 9, and 12 were used for the acquisition of the *b*-values of 0, 100, 500, 1000, and 1200, respectively.

^bEcho times of 13, 26, 40, 53, 66, 79, 92, and 105 were used.

acquired. The number of slices was adjusted to cover the entire specimen. T1 relaxation times were measured using a series of spoiled gradient echo sequences with a fixed repetition time and increasing flip angles of 2°, 5°, 12°, and 20°. T2 relaxation times were measured using a single-slice spin echo sequence with an echo spacing of 13 ms and a total number of eight echoes.

2.3 | Histological processing and annotation of tumor-free margins

Following MRI acquisition, the container with the specimen was transported to the pathology laboratory for formalin fixation. Next, the specimen was completely cut in 4 mm thick slices and whole-mount paraffin embedded.

From each of the paraffin blocks, a 4 μm slice was obtained and stained with hematoxylin and eosin. The histological slides were digitalized.¹⁸ A dedicated head and neck pathologist (AvE) without knowledge of the MRI annotated OSCC location and the three minimal tumor-free margins, that is, both minimal lateral margins at 9-o'clock and 3-o'clock and one deep margin, for each available slide where appropriate. The height and width of the specimen were determined on the middlemost slide. Furthermore, the TNM classification, depth of invasion, maximum tumor diameter, and presence of unfavorable growth patterns were reported.

2.4 | Qualitative and quantitative analysis

For the qualitative analysis, two radiologists (SS, dedicated head and neck radiologist; and JF, dedicated to body MRI applications), R1 and R2, scored the image quality of the acquired MRI series using the following 5-point scale¹⁹: 1, very poor nondiagnostic quality images; 2, low image quality that degraded confidence in diagnosis; 3, moderate image quality sufficient for diagnosis; 4, good image quality; 5, excellent image quality enabling visualization of even small structures. Furthermore, OSCC visibility and visibility of the start of the resection plane, that is, the point where the mucosal surface ends and the surgeon started excising were scored as 1, very poor; 2, poor; 3, sufficient; 4, good; or 5, excellent.

For the quantitative T1 maps, the obtained signal curves were linearized and T1 relaxation times were computed by linear least square fits on the transformed data.²⁰ T2 relaxation times were computed by fitting the monoexponential decay curves on the MR signal magnitude as a function of echo time, discarding the first echo to reduce the effect of refocusing flip angle imperfections. Mean T1 and T2 relaxation times, and ADC values were calculated within regions of interest (ROI) drawn on the OSCC and surrounding healthy tissue.

2.5 | Annotation of tumor-free margins on MRI

The MRI series that had the highest image quality was matched to histology and subsequently used for annotations. An observer (JH) matched individual MRI slices to each of the obtained histological slides by employing the fact that every few MRI slices an MRI slice corresponds with a histological slide. The degree to which an MRI slice matched to the histological slide was inspected for

corresponding contours and shapes as well as anatomical landmarks. The height and width of the specimen were measured on MRI at identical positions as on histology. During a single session, the pathologist instructed the two radiologists on the way tumor-free margins are determined under the microscope using representative histological slides from patients not related to this study. Next, both readers individually annotated OSCC location and the minimal tumor-free margins where appropriate but without knowledge of the gold standard. Annotation was performed on a dedicated workstation developed in MATLAB (version R2014b, MathWorks, Natick, Massachusetts) that applied a timestamp on each of the annotated images, enabling subsequent computation of annotation times.

2.6 | Statistical analysis

The MRI annotations were corrected for shrinkage with the mean formalin fixation induced shrinkage factor as the ratio between height and width measurements of the specimen on MRI and histology.¹⁸ The correlation and agreement between MRI and histology annotations as well as between the two readers were determined by calculating Spearman's correlation coefficients and performing Bland-Altman analysis, respectively. The diagnostic performance of MRI in localizing OSCC and identifying margins less than 5 mm was assessed by calculating sensitivity, specificity, and positive and negative predictive values (PPV, NPV). Correct annotation of OSCC presence and identification of a margin less than 5 mm were considered true positives, while correct annotation of OSCC absence and identification of a margin larger than or equal to 5 mm were true negatives. The Dice similarity coefficient (DSC) was computed to determine the spatial overlap of the cancer area annotations between the two readers. Furthermore, the agreement between the two readers was evaluated by computing proportions of positive and negative agreement (PA, NA) as proposed by de Vet et al.²¹

3 | RESULTS

Ten patients were included between October 2017 and December 2018 (Table 2). Of 10 specimens, 105 histological slides were obtained of which 58 contained OSCC. One anterior tongue tip specimen was included that inherently contained only a single resection plane, consequently seven 3-o'clock and deep margins were not present. In total, 58 9-o'clock margins, 51 3-o'clock, and 51 deep margins were annotated on histology of

TABLE 2 Clinical and histological characteristics of study cohort (n = 10)

Characteristics	Value
Age (y), median (range)	58 (32-86)
Clinical TNM classification, No. of patients	
cT1	2
cT2	4
cT2N1	1
cT3	2
cT4aN2b	1
SNP, No. of patients	7
ND, No. of patients	4
Specimen dimensions (l × w × h, cm), range	3.2 × 2.5 × 1.5 to 5.0 × 5.4 × 2.6
Pathological TNM classification, No. of patients	
pT1	4
pT1N1	1
pT2	1
pT3	2
pT4aN2b	2
Invasion depth (cm), median (range)	0.8 (0.1-1.7)
Maximum tumor diameter (cm), median (range)	2.15 (0.2-3.6)
Tumor-free margin status, No. of patients	
<5 mm	3
>5 mm	7
Unfavorable grow pattern, No. of patients	6
Postoperative management, No. of patients	
Follow-up	6
Radiotherapy	4

Abbreviations: ND, neck dissection; SNP, sentinel node procedure.

which 5, 6, and 6 margins were less than 5 mm, respectively.

3.1 | Qualitative and quantitative analysis

The T2 TSE TE12 (hereafter referred to as T2) and b1000/ADC-map had the highest image quality scores, *good to excellent* (Figure 2). OSCC was best visible on the b1000 series and ADC-map (*good to excellent*) while the T2 had the highest score (*good*) for visibility of the start of the resection plane. The T2 series was therefore the series that was matched to histology and was subsequently annotated. The readers only used the b1000 and the ADC-map in conjunction to annotating the T2 series, the rest of MRI series was discarded.

ROIs on OSCC and healthy tissue were drawn in seven of the 10 specimens. In three specimens, the OSCC area was considered too small for reliable ROI positioning. Median T1-times for normal and OSCC tissue of 1429 ms and 1415 ms were, respectively, observed. The median T2-times were 86.7 ms and 95.4 ms, and ADC values were 1103 $\mu\text{m}^2/\text{s}$ and 609 $\mu\text{m}^2/\text{s}$ for normal and OSCC tissue (Figure 3).

3.2 | Correlation and agreement between MRI and histology

Each histological slide was matched to a corresponding MRI slice (Figures 4 and 5). The margin annotations on MRI were corrected with a mean factor of 0.89 (95% confidence interval [95% CI] = 0.85-0.93) and the OSCC area with a mean factor of 0.80 (the square of 0.89) due to its

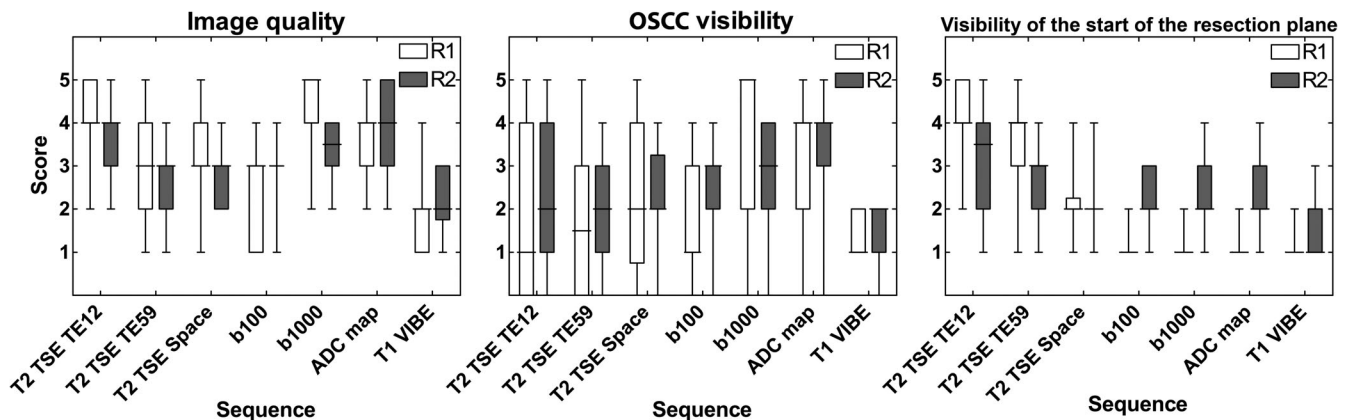


FIGURE 2 Results of qualitative image evaluation represented in box-whisker plots for readers R1 (nonfilled boxes) and R2 (gray filled boxes), with the results for Image quality, OSCC visibility, and Visibility of the start of the resection plane. The box plots demonstrate the median score (bold horizontal lines), interquartile range (boxes), and extreme values (whiskers). OSCC, oral squamous-cell carcinoma

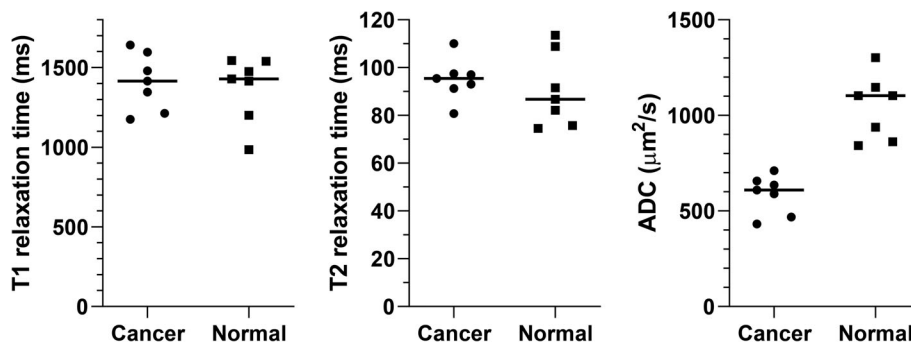


FIGURE 3 Median and individual ($n = 7$) T1, T2, and ADC values for OSCC and healthy tongue tissue. ADC, apparent diffusion coefficient; OSCC, oral squamous-cell carcinoma

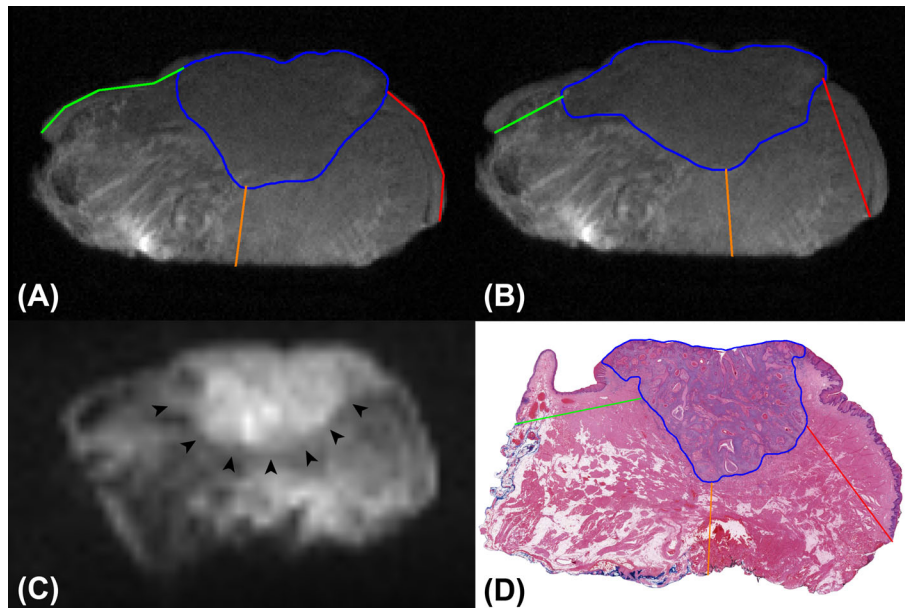


FIGURE 4 Example of MR images and corresponding histological slide obtained from a tongue resection specimen from an 86-year-old female patient. Blue lines, annotations of OSCC; green, 9-o'clock margin; orange, deep margin; red, 3-o'clock margin. The DSC between the annotated OSCC areas on MRI was 0.87 for this case. A, Annotation by reader 1 of MR image obtained with a T2W TSE sequence. OSCC area = 107 mm²; 9-o'clock margin = 11.6 mm; deep margin = 5.7 mm; 3-o'clock margin = 10.7 mm. B, Annotation by reader 2 of identical MR image as (A). OSCC area = 114 mm²; 9-o'clock margin = 5.5 mm; deep margin = 6.2 mm; 3-o'clock margin = 10.5 mm. At 9-o'clock side, the OSCC area appears overestimated resulting in underestimation of the 9-o'clock margin. C, Corresponding diffusion weighted b1000 image showing diffusion restriction (black arrowheads). D, Corresponding hematoxylin and eosin stained histological slide at $\times 100$ magnification confirmed a pT3 OSCC. OSCC area = 79 mm²; 9-o'clock margin = 8.4 mm; deep margin = 6.1 mm; 3-o'clock margin = 9.4 mm. DSC, Dice similarity coefficient; OSCC, oral squamous-cell carcinoma; TSE, turbo spin echo [Color figure can be viewed at wileyonlinelibrary.com]

two-dimensionality. The median annotation time for R1 was 03'45" (range 00'13"-11'32") and for R2 04'40" (range 00'11-26'18").

Reader R1 annotated presence of OSCC in 45 MRI slices of which 43 were in agreement with histology (PPV 96%; 95% CI = 90%-100%; Tables 3 and 4). In the 43 true positive (TP) slices, a total of 13 margins were evaluated as less than 5 mm, of which 5 were in accordance with histology (PPV 38%; 95% CI = 12%-65%), and 104 margins were evaluated as 5 mm or greater, of which 95 were in accordance with histology (NPV 91%; 95% CI = 86%-

97%). Reader R2 annotated presence of OSCC in 52 MRI slices of which 45 were in agreement with histology (PPV 87%; 95% CI = 77%-96%). In two slices, R2 indicated OSCC presence on MRI but at a location completely different from histology and were therefore considered false positives (FPs). Based on 45 TP slices, the PPV and NPV of R2 for identifying margins less than 5 mm were 0% (0/15) and 87% (92/106; 95% CI = 80%-93%). R1 and R2 both failed to detect one pT1 case of biopsy-proven OSCC, which only contained severe dysplasia (maximum diameter = 0.4 cm) on final histopathology of the

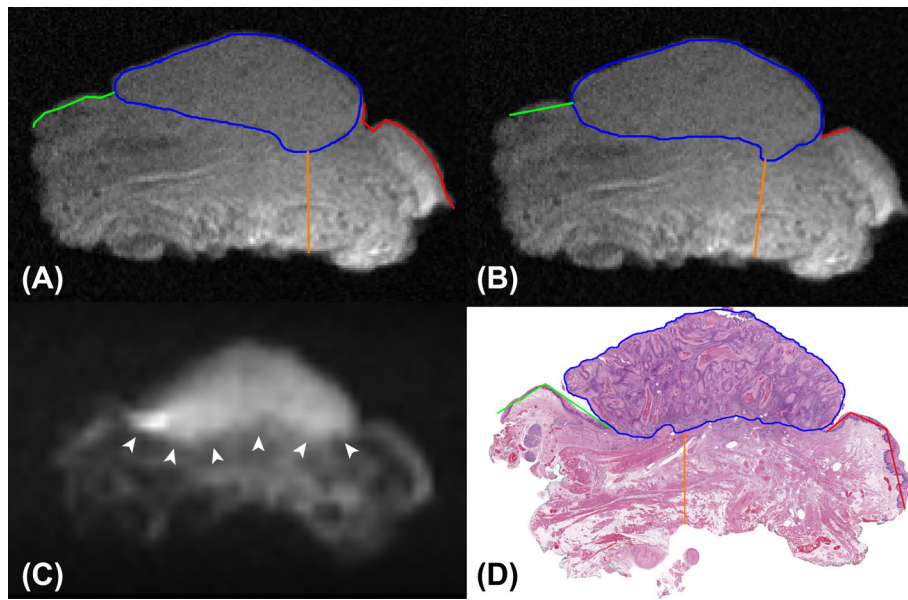


FIGURE 5 Example of MR images and corresponding histological slide obtained from a tongue resection specimen from an 82-year-old male patient. Blue lines, annotations of OSCC; green, 9-o'clock margin; orange, deep margin; red, 3-o'clock margin. The DSC between the annotated OSCC areas on MRI was 0.92 in this case. Note that on the histological slide a sulcus is present on both sides of the exofytically growing tumor that are not visible on MRI. A, Annotation by reader 1 of MR image obtained with a T2W TSE sequence. OSCC area = 95 mm²; 9-o'clock margin = 6.6 mm; deep margin = 7.3 mm; 3-o'clock margin = 11.3 mm. B, Annotation by reader 2 of identical MR image as (A). OSCC area = 105 mm²; 9-o'clock margin = 4.6 mm; deep margin = 7.0 mm; 3-o'clock margin = 4.6 mm. Both the 9- o'clock and 3-o'clock margins were false positively evaluated as less than 5 mm which was probably caused by difficulties in determining the point where the healthy mucosa ends and where the resection plane start. C, Corresponding diffusion weighted b1000 image showing diffusion restriction (white arrowheads). D, Corresponding hematoxylin and eosin stained histological slide at ×100 magnification confirmed a pT2 OSCC. OSCC area = 114 mm²; 9-o'clock = 9.3 mm; deep margin = 6.4 mm; 3-o'clock margin = 10.6 mm. DSC, Dice similarity coefficient; OSCC, oral squamous-cell carcinoma; TSE, turbo spin echo [Color figure can be viewed at wileyonlinelibrary.com]

TABLE 3 Diagnostic accuracy of reader 1 and reader 2 in localizing oral squamous-cell carcinoma on MRI and proportions of positive and negative agreement

	Reader 1	Reader 2
n/N (sensitivity, 95% CI)	43/58 (0.74, 0.63-0.85)	45/56 (0.80, 0.70-0.91)
n/N (PPV, 95% CI)	43/45 (0.96, 0.90-1)	45/52 (0.87, 0.77-0.96)
2TP/(2TP + FN + FP), (PA, 95% CI)	2 × 41/(2 × 41 + 4 + 9), (0.86, 0.77-0.95)	
n/N (specificity, 95% CI)	45/47 (0.96, 0.90-1)	42/49 (0.86, 0.76-0.96)
n/N (NPV, 95% CI)	45/60 (0.75, 0.64-0.86)	42/53 (0.79, 0.68-0.90)
2TN/(2TN + FN + FP), (NA, 95% CI)	2 × 51/(2 × 51 + 4 + 9), (0.88, 0.81-0.96)	

Note: Reader 2 was penalized with two false positives for annotating tumor on two MRI slices that had corresponding histological slides that contained tumor but at a completely different location.

Abbreviations: CI, confidence interval; FN, false negative; FP, false positive; NA, proportion of negative agreement; NPV, negative predictive values; PA, proportion of positive agreement; PPV, positive predictive values; TN, true negative; TP, true positive.

resected specimen. R1 missed one pT1 case of severe dysplasia containing some fields of invasive cancer (maximum diameter = 0.4 cm).

The OSCC area annotations of both readers showed a positive correlation with histology (R1, 0.82; R2, 0.82; Figures S1 and S2). Bland-Altman analysis revealed that

both readers overestimated the OSCC area compared to histology, with a tendency toward larger overestimation at larger mean OSCC areas. Positive correlations, ranging from 0.12 to 0.71, were observed for the margin annotations of both readers. R1 showed a mean overestimation of 2.5 mm and 2.2 mm for the 9- o'clock and 3-o'clock

TABLE 4 Diagnostic accuracy of reader 1 and reader 2 in identifying margins less than 5 mm on MRI and proportions of positive and negative agreement

	3-o'clock margin	9-o'clock margin	Deep margin	Margins combined
Reader 1				
<5 mm, n/N (sensitivity, 95% CI)	2/4 (0.5, 0.01-0.99)	0/5 (0, 0-0)	3/5 (0.21, 0.17-1)	5/14 (0.36, 0.11-0.61)
≥5 mm, n/N (specificity, 95% CI)	30/33 (0.91, 0.81-1)	35/38 (0.92, 0.85-1)	30/32 (0.94, 0.85-1)	95/103 (0.92, 0.87-0.97)
<5 mm, n/N (PPV, 95% CI)	2/5 (0.4, 0-0.83)	0/3 (0, 0-0)	3/5 (0.6, 0.17-1)	5/13 (0.38, 0.12-0.65)
≥5 mm, n/N (NPV, 95% CI)	30/32 (0.94, 0.85-1)	35/40 (0.88, 0.77-0.98)	30/32 (0.94, 0.85-1)	95/104 (0.91, 0.86-0.97)
Reader 2				
<5 mm, n/N (sensitivity, 95% CI)	0/4 (0, 0-0)	0/5 (0, 0-0)	1/5 (0.2, 0-0.55)	1/14 (0.07, 0-0.21)
≥5 mm, n/N (specificity, 95% CI)	27/34 (0.79, 0.66-0.93)	34/40 (0.85, 0.74-0.96)	26/33 (0.79, 0.65-0.93)	87/107 (0.81, 0.74-0.89)
<5 mm, n/N (PPV, 95% CI)	0/7 (0, 0-0)	0/6 (0, 0-0)	1/8 (0.13, 0-0.35)	1/21 (0.05, 0-0.14)
≥5 mm, n/N (NPV, 95% CI)	27/31 (0.87, 0.75-0.99)	34/39 (0.87, 0.77-0.98)	26/30 (0.87, 0.75-0.99)	87/100 (0.87, 0.80-0.93)
Proportions of agreement				
<5 mm, 2TP/(2TP + FN + FP) (PA, 95% CI)	$2 \times 1 / (2 \times 1 + 4 + 3)$ (0.22, 0-0.51)	$2 \times 2 / (2 \times 2 + 0 + 4)$ (0.5, 0.10-0.90)	$2 \times 2 / (2 \times 2 + 3 + 4)$ (0.36, 0.05-0.68)	$2 \times 5 / (2 \times 5 + 7 + 11)$ (0.36, 0.16-0.55)
≥5 mm, 2TN/(2TN + FN + FP) (NA, 95% CI)	$2 \times 27 / (2 \times 27 + 4 + 3)$ (0.89, 0.79-0.99)	$2 \times 35 / (2 \times 35 + 0 + 4)$ (0.96, 0.87-1)	$2 \times 26 / (2 \times 26 + 3 + 4)$ (0.88, 0.77-0.99)	$2 \times 88 / (2 \times 88 + 7 + 11)$ (0.91, 0.85-0.96)

Abbreviations: CI, confidence interval; FN, false negative; FP, false positive; NA, proportion of negative agreement; NPV, negative predictive values; PA, proportion of positive agreement; PPV, positive predictive values; TN, true negative; TP, true positive.

margin, respectively, whereas the annotations by R2 show mean biases of nearly 0 (0.6 mm and -0.9 mm, respectively). Both readers underestimated the deep margin by -1.4 mm on average. The 95% limits of agreement for both the lateral margins were wider than for the deep margin. There was no apparent trend for margin size.

3.3 | Correlation and agreement between the R1 and R2

The OSCC area annotations of both readers were strongly correlated (0.92; Figure S3). A mean bias of 10.6 mm² between R2 and R1 was observed. The mean DSC was 0.80 (95% CI = 0.76-0.85). Both readers indicated OSCC presence in 41 MRI slices (TP), OSCC absence in 51 (true negative [TN]). In 4 slices R1 indicated OSCC presence while R2 indicated absence (false negative [FN]), and in 9 this was vice versa (FP). This resulted in a PA of 86% (95% CI = 77%-95%) and an NA of 88% (95% CI = 81%-96%). The 9- o'clock and 3-o'clock margin annotations were less strongly correlated (0.55 and 0.15, respectively)

and showed mean biases between R2 and R1 of -2.1 mm and -1.8 mm. For the deep margin, the mean bias was almost zero with narrower 95% limits of agreement and a stronger correlation (0.71) compared to the two lateral margins. The PA and NA for the three margins combined were 36% (95% CI = 16%-55%) and 91% (95% CI = 85%-96%). This was based on 5 margins annotated as less than 5 mm by both readers (TP), 88 margins annotated a larger than 5 mm by both readers (TN), and 7 (FN) and 11 (FP) margins that were annotated as less than 5 mm by R1 and larger than 5 mm by R2, and vice versa.

4 | DISCUSSION

Our results demonstrated that the T2 weighted images provided the highest image quality, and that the diffusion weighted images provided the highest contrast between OSCC and healthy tissue in fresh tongue specimens imaged on a 3 T clinical MRI. MRI demonstrated high diagnostic performance in OSCC localization and high inter-reader agreement. The specificity of MRI in

identifying margins less than 5 mm was high, its sensitivity was however poor.

Several techniques aiming for intraoperative assessment of surgical margins in oral cavity/tongue squamous cell carcinoma have been investigated such as elastic scattering spectroscopy,²² fluorescence,²³⁻²⁵ hyperspectral imaging,²⁶ optical coherence tomography,²⁷ Raman spectroscopy,²⁸ and ultrasound.²⁹ Some of the techniques have advantages over MRI by providing higher resolutions²⁷ or shorter acquisition times^{22,27,29} but are limited in sampling the entire specimen^{22,23,26,28} and/or probing depth^{22,27} compared to MRI. In contrast to our study, some authors^{22,23,26} observed higher diagnostic accuracies, but they employed a case-control study design, that is, the techniques were assayed for discrimination between samples of tumor and healthy tissue, thereby limiting the (clinical) implications of their results. The study by Van Keulen et al²⁴ used a targeted fluorescence agent to identify where tumor is located closest to the deep surface of the specimen. Similar to our study, Hamdoon et al²⁷ assessed surgical margins in entire specimens, but they only focused on detecting involved (positive) margins, that is, tumor reaching the inked margin. Although Tarabichi et al²⁹ did measure the tumor-free margin, that is, the thickness of uninvolved healthy tissue surrounding the tumor, rather than focusing on margin involvement alone, they did not directly compare the ultrasound measurements to histology and therefore diagnostic accuracy cannot be assessed.

Compared to previous work, several limitations were resolved.¹⁷ First, the logistics were optimized. Instead of walking great distances between the OR, department of pathology, and MRI scanner, specimen preparation and scanning were all performed in the OR suite which saved time. Second, the clinical 3 T MRI scanner using off-the-shelf receiver coils substituted costly and not widely available 7 T MRI equipment. Third, although the diagnostic performance of our method in identifying margins less than 5 mm was weak, we showed that it is feasible to perform MRI acquisition (approximately 15 minutes for T2W and diffusion-weighted images) and radiological evaluation within a clinically realistic time frame of under 30 minutes, which is comparable to FSA.¹⁵ Finally, the nonblinded study design was adapted to a stronger blinded design with two independent readers unaware of the gold standard.

Our method might be subject of further investigations. The changeover to a clinical 3 T MRI system resolved some limitations, but at the expense of the signal to noise ratio (SNR). Although the voxel sizes and measurement times were larger and longer than at 7 T,¹⁷ we assume that this did not completely compensate the SNR losses. Consequently, this might have hampered

visualization of fine details, such as the transition between the mucosa and the resection plane. Another fine detail that was difficult to observe on MRI, were the sulci present in specimens with exophytic tumors. In case of a sulcus, that is, where the exophytic part of the tumor extended over the healthy mucosa, the healthy mucosa and tumor were sometimes indistinguishable on MRI. The sensitivity of MRI could be improved if the transition between the resection plane and healthy mucosa as well as the location of sulci could be marked.

Some limitations should be discussed. First, the sample size was small and heterogeneous. Our cohort contained a broad range of cases with various T classifications, half of which were (small) classification pT1 that bear the lowest risk of having inadequate margins.⁶ Furthermore, a relatively small proportion of the margins were less than 5 mm. As a result, our study might unintentionally have emphasized on identifying margins larger than 5 mm, rather than identifying margins less than 5 mm. It could therefore be interesting to further investigate the performance of our method in recreated close margins in orthotopic xenograft tumor models. A second limitation is the inexperience of the readers. Both readers were experienced with in vivo applications of MRI, but now had to evaluate histopathological features in images of ex vivo tongue resection specimens. Therefore, a learning curve might have affected the readers' evaluation. A third limitation is the fact that only one pathologist evaluated histopathology. Although the inter-reader variability for evaluating the resection margin itself has not been investigated, the agreement in scoring other pathological features in OSCC is moderate.^{30,31} Therefore, the reproducibility of the adhered gold standard itself might be questionable.

The surgeon has to keep the balance between performing radical surgery and maintaining functionality while operating within complex anatomy. The high incidence rates of inadequate resection margins in tongue/oral cancer surgery prove that intraoperative methods of visual inspection and palpation are limited in assessing the surgical resection margins.^{6,9,14} The major drawback of intraoperative FSA is its susceptibility to sampling errors and its ability to prevent inadequate surgical margins is therefore questionable.^{15,16,32} Moreover, the technique is not cost-effective.¹⁵ There is therefore a need for techniques that are able to detect inadequate surgical margins. Several (imaging) techniques have been investigated for this purpose that show promising results, but none have yet established a permanent role within clinical practice. We presented a method already close to an envisioned future clinical application that was able to satisfy two prerequisites for accurate prediction of the surgical margin status, namely sampling of entire fresh tongue specimens with high quality images and accurate

localization of OSCC. However, given its poor sensitivity in identifying margins less than 5 mm, MRI is not yet ready for clinical practice. Further investigations should point out if the sensitivity of MRI could be increased so that the technique may ultimately reduce the number of patients that leave the hospital with inadequate margins.

5 | CONCLUSION

Accurate localization of OSCC with high inter-reader agreement in fresh tongue resection specimens using a 3 T clinical MRI scanner is possible. It seems however not yet feasible to accurately assess the surgical margin status with MRI.

ORCID

Jan Heidkamp  <https://orcid.org/0000-0002-3335-1486>
Robert P. Takes  <https://orcid.org/0000-0003-4784-0499>

REFERENCES

- Siegel RL, Miller KD, Jemal A. Cancer statistics, 2018. *CA Cancer J Clin*. 2018;68(1):7-30.
- Bell RB, Kademani D, Homer L, Dierks EJ, Potter BE. Tongue cancer: is there a difference in survival compared with other subsites in the oral cavity? *J Oral Maxillofac Surg*. 2007;65(2):229-236.
- Yao M, Epstein JB, Modi BJ, Pytynia KB, Mundt AJ, Feldman LE. Current surgical treatment of squamous cell carcinoma of the head and neck. *Oral Oncol*. 2007;43(3):213-223.
- National Comprehensive Cancer Network. NCCN Clinical Practice Guidelines in Oncology, Head and Neck Cancer, Version 2.2013 [Internet]. https://www.nccn.org/professionals/physician_gls/pdf/head-and-neck.pdf. Accessed May 8, 2018.
- Slootweg PJ, Hordijk GJ, Schade Y, van Es RJJ, Koole R. Treatment failure and margin status in head and neck cancer. A critical view on the potential value of molecular pathology. *Oral Oncol*. 2002;38(5):500-503.
- Sutton DN, Brown JS, Rogers SN, Vaughan ED, Woolgar JA. The prognostic implications of the surgical margin in oral squamous cell carcinoma. *Int J Oral Maxillofac Surg*. 2003;32(1):30-34.
- Binahmed A, Nason RW, Abdoh AA. The clinical significance of the positive surgical margin in oral cancer. *Oral Oncol*. 2007;43(8):780-784.
- Chen TC, Wang CP, Ko JY, Yang TL, Lou PJ. The impact of pathologic close margin on the survival of patients with early stage oral squamous cell carcinoma. *Oral Oncol*. 2012;48(7):623-628.
- Smits RWH, Koljenović S, Hardillo JA, et al. Resection margins in oral cancer surgery: room for improvement. *Head Neck*. 2016;38(suppl 1):E2197-E2203.
- Helliwell T, Woolgar J. *Standards and Datasets for Reporting Cancers. Dataset for Histopathology Reporting of Mucosal Malignancies of the Oral Cavity*. London: Royal College of Pathologists; 2013.
- Hinni ML, Ferlito A, Brandwein-Gensler MS, et al. Surgical margins in head and neck cancer: a contemporary review. *Head Neck*. 2013;35(9):1362-1370.
- Langendijk JA, Ferlito A, Takes RP, et al. Postoperative strategies after primary surgery for squamous cell carcinoma of the head and neck. *Oral Oncol*. 2010;46(8):577-585.
- Kouloulis V, Thalassinou S, Platoni K, et al. The treatment outcome and radiation-induced toxicity for patients with head and neck carcinoma in the IMRT era: a systematic review with dosimetric and clinical parameters. *Biomed Res Int*. 2013;2013:401261.
- Kerker FA, Adler W, Brunner K, et al. Anatomical locations in the oral cavity where surgical resections of oral squamous cell carcinomas are associated with a close or positive margin—a retrospective study. *Clin Oral Investig*. 2018;22(4):1625-1630.
- DiNardo LJ, Lin J, Karageorge LS, Powers CN. Accuracy, utility, and cost of frozen section margins in head and neck cancer surgery. *Laryngoscope*. 2000;110(10):1773-1776.
- Gerber S, Gengler C, Grätz KW, Kruse AL. The impact of frozen sections on final surgical margins in squamous cell carcinoma of the oral cavity and lips: a retrospective analysis over an 11 years period. *Head Neck Oncol*. 2011;3(1):56.
- Steens SCA, Bekers EM, Weijis WLJ, et al. Evaluation of tongue squamous cell carcinoma resection margins using ex-vivo MR. *Int J Comput Assist Radiol Surg*. 2017;12(5):821-828.
- Heidkamp J, Zusterzeel PLM, van Engen-van Grunsven ACH, et al. MRI evaluation of vulvar squamous-cell carcinoma in fresh radical local excision specimens for cancer localization and prediction of surgical tumor-free margins. *NMR Biomed*. 2019;32(1):1-12.
- Schueller-Weidekamm C, Schaefer-Prokop CM, Weber M, Herold CJ, Prokop M. CT angiography of pulmonary arteries to detect pulmonary embolism: improvement of vascular enhancement with low kilovoltage settings. *Radiology*. 2006;241(3):899-907.
- Fram EK, Herfkens RJ, Johnson GA, et al. Rapid calculation of T1 using variable flip angle gradient refocused imaging. *Magn Reson Imaging*. 1987;5(3):201-208.
- de Vet HCW, Mookink LB, Terwee CB, Hoekstra OS, Knol DL. Clinicians are right not to like Cohen's κ . *BMJ*. 2013;346(April):1-7.
- Grillone GA, Wang Z, Krisciunas GP, et al. The color of cancer: margin guidance for oral cancer resection using elastic scattering spectroscopy. *Laryngoscope*. 2017;127(suppl 4):S1-S9.
- Warram JM, de Boer E, van Dam GM, et al. Fluorescence imaging to localize head and neck squamous cell carcinoma for enhanced pathological assessment. *J Pathol Clin Res*. 2016;2(2):104-112.
- Van Keulen S, Nishio N, Birkeland A, et al. The sentinel margin: intraoperative ex vivo specimen mapping using relative fluorescence intensity. *Clin Cancer Res*. 2019;25(15):4656-4662.
- Gao RW, Teraphongphom NT, van den Berg NS, et al. Determination of tumor margins with surgical specimen mapping using near-infrared fluorescence. *Cancer Res*. 2018;78(17):5144-5154.
- Fei B, Lu G, Wang X, et al. Label-free reflectance hyperspectral imaging for tumor margin assessment: a pilot study on surgical specimens of cancer patients. *J Biomed Opt*. 2017;22(8):1-7.

27. Hamdoon Z, Jerjes W, McKenzie G, Jay A, Hopper C. Optical coherence tomography in the assessment of oral squamous cell carcinoma resection margins. *Photodiagnosis Photodyn Ther*. 2016;13:211-217.
28. Barroso EM, Smits RWH, Van Lanschot CGF, et al. Water concentration analysis by Raman spectroscopy to determine the location of the tumor border in oral cancer surgery. *Cancer Res*. 2016;76(20):5945-5953.
29. Tarabichi O, Kanumuri V, Juliano AF, Faquin WC, Cunnane ME, Varvares MA. Intraoperative ultrasound in oral tongue cancer resection: feasibility study and early outcomes. *Otolaryngol Head Neck Surg*. 2018;158(4):645-648.
30. Sawairz FA, Irwin CR, Gordon DJ, Leonard AG, Stephenson M, Napier SS. Invasive front grading: reliability and usefulness in the management of oral squamous cell carcinoma. *J Oral Pathol Med*. 2003;32(1):1-9.
31. Heerema MGJ, Melchers LJ, Roodenburg JLN, Schuurin E, de Bock GH, van der Vegt B. Reproducibility and prognostic value of pattern of invasion scoring in low-stage oral squamous cell carcinoma. *Histopathology*. 2016;68(3):388-397.
32. Pathak KA, Nason RW, Penner C, Viallet NR, Sutherland D, Kerr PD. Impact of use of frozen section assessment of operative margins on survival in oral cancer. *Oral Surg Oral Med Oral Pathol Oral Radiol Endod*. 2009;107(2):235-239.

SUPPORTING INFORMATION

Additional supporting information may be found online in the Supporting Information section at the end of this article.

How to cite this article: Heidkamp J, Weijs WLJ, van Engen-van Grunsven ACH, et al. Assessment of surgical tumor-free resection margins in fresh squamous-cell carcinoma resection specimens of the tongue using a clinical MRI system. *Head & Neck*. 2020;42:2039–2049. <https://doi.org/10.1002/hed.26125>